

Figure S1. (a)  $^1\text{H}$  NMR spectrum of PLA-CTA (400 MHz,  $\text{CDCl}_3$ , 20  $^\circ\text{C}$ ). The inset shows a magnified spectrum of PLA-CTA in the range of 3-5 ppm used for  $M_n$  determination by end group analysis. (b) SEC trace of PLA-CTA (chloroform, 35  $^\circ\text{C}$ , 1  $\text{mL min}^{-1}$ , RI detector).

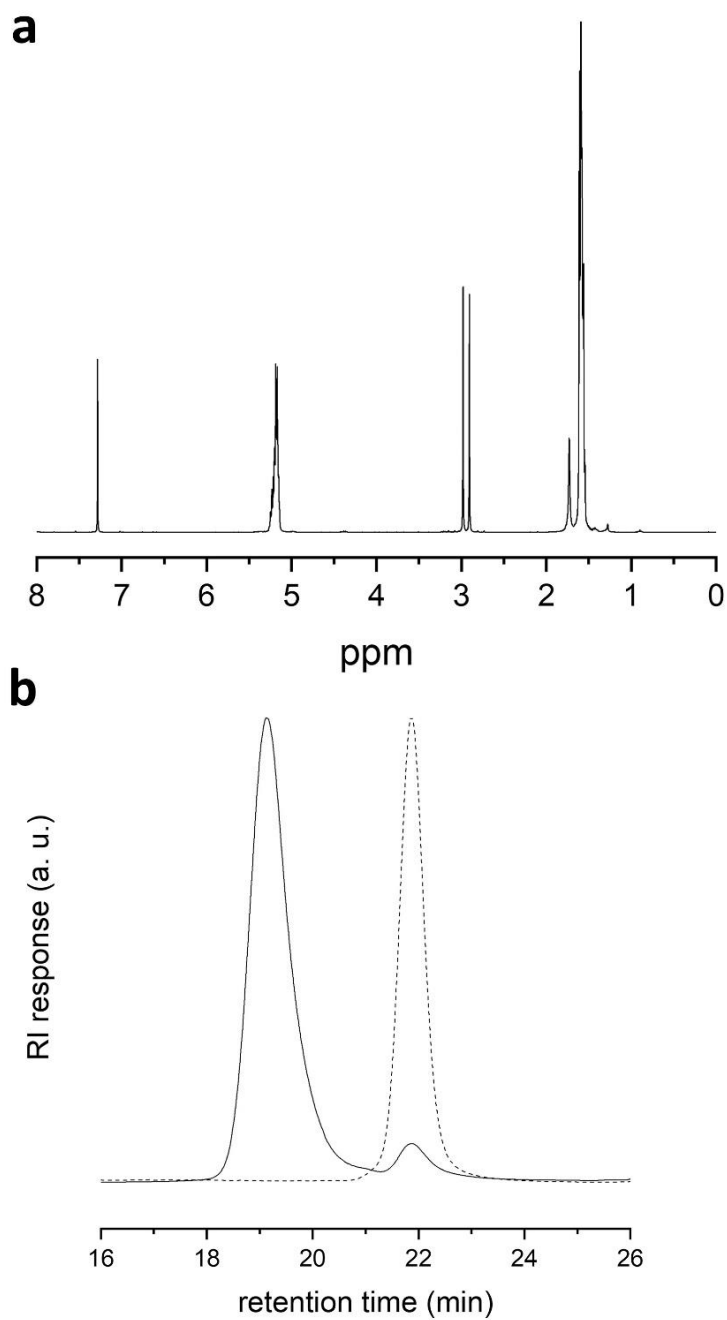


Figure S2. (a)  $^1\text{H}$  NMR spectrum of  $\text{PLA}_n$  (400 MHz,  $\text{CDCl}_3$ , 20  $^\circ\text{C}$ ). (b) SEC traces of  $\text{PLA}_n$  (solid line) and  $\text{PLA-CTA}$  (dashed line). The traces were recorded with a RI detector using chloroform as eluent at 35  $^\circ\text{C}$  with flow rate of 1  $\text{mL min}^{-1}$ .

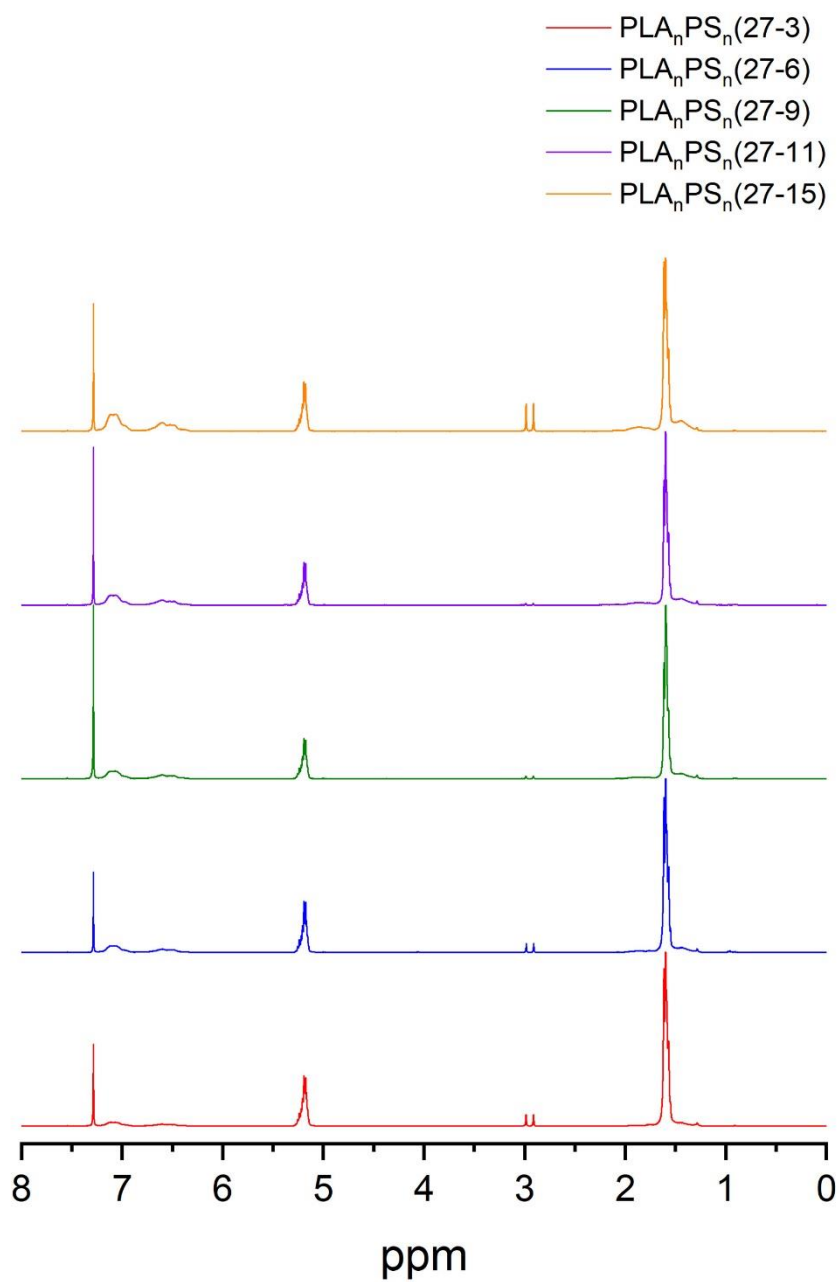


Figure S3. <sup>1</sup>H NMR spectra of PLA<sub>n</sub>PS<sub>n</sub> obtained with different polymerization time via in-out approach (400 MHz, CDCl<sub>3</sub>, 20 °C). Two small singlets appearing at 3.0 – 2.8 ppm originate from residual DMF which was the reaction solvent.

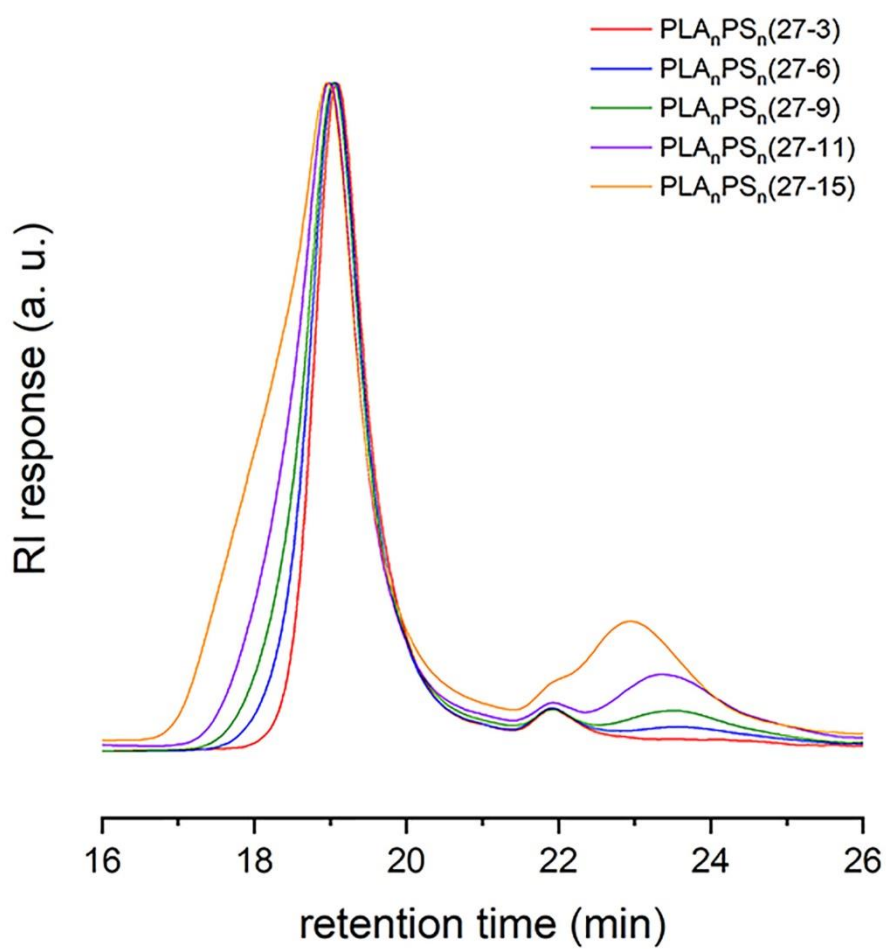


Figure S4. SEC overlay of PLA<sub>n</sub>PS<sub>n</sub> obtained with different polymerization time via in-out approach prior to purification.

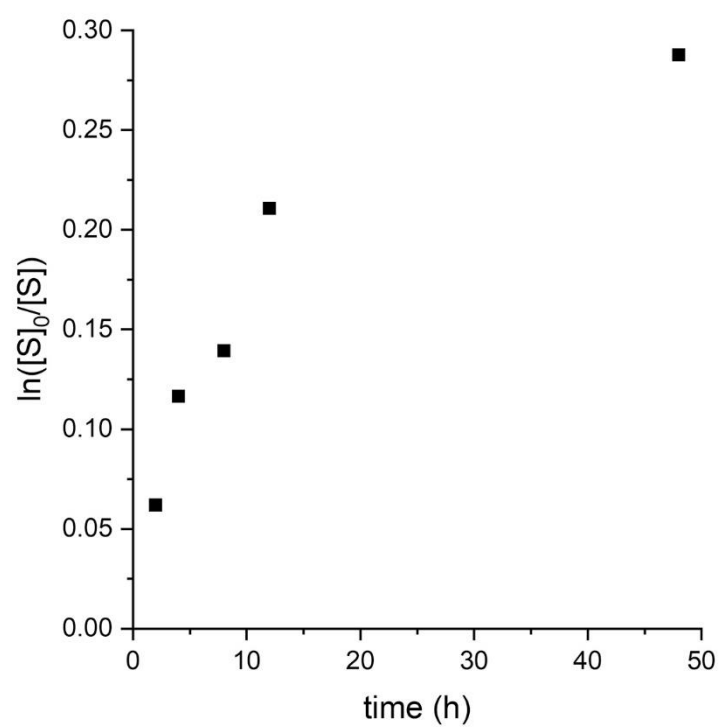


Figure S5. First-order kinetic plot with respect to styrene concentration.

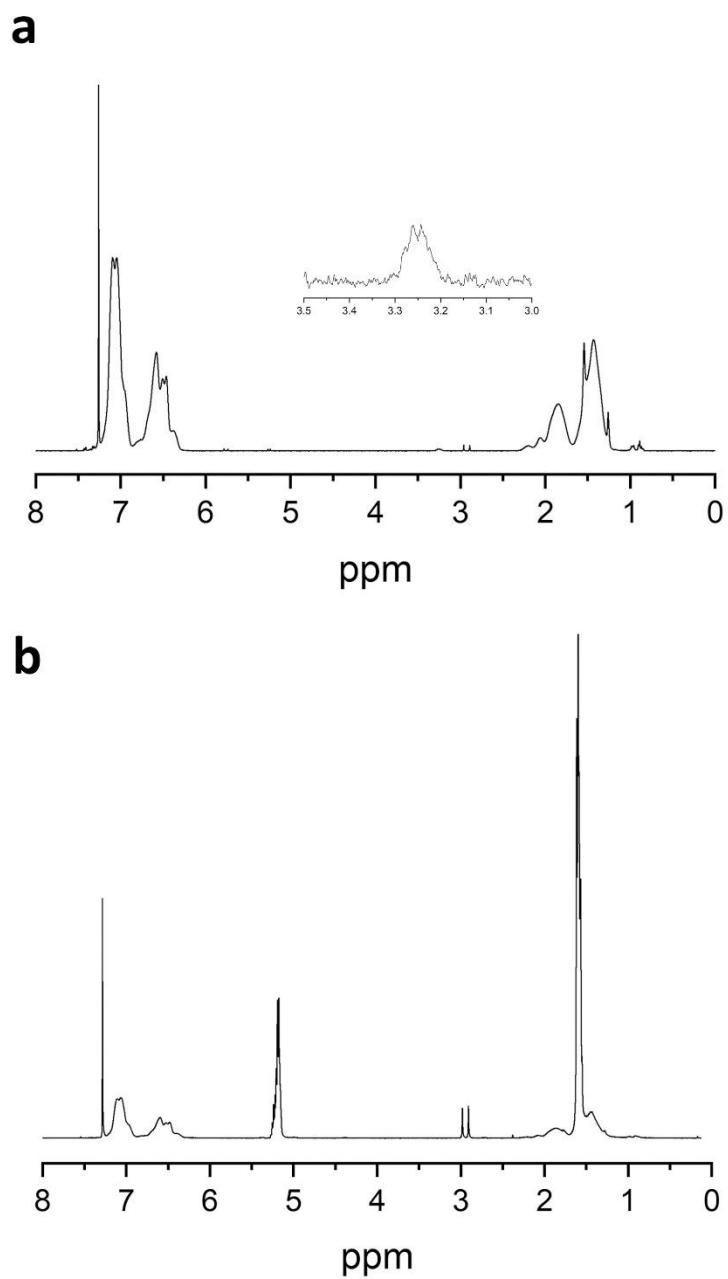


Figure S6.  $^1\text{H}$  NMR spectra of (a) PS-CTA and (b)  $\text{PLA}_n\text{PS}_n(27-13)\text{-Multi MI}$  (400 MHz,  $\text{CDCl}_3$ , 20  $^\circ\text{C}$ ). The inset in a shows a magnified spectrum of PS-CTA in the range of 3.2-3.3 ppm used for  $M_n$  determination by end group analysis.

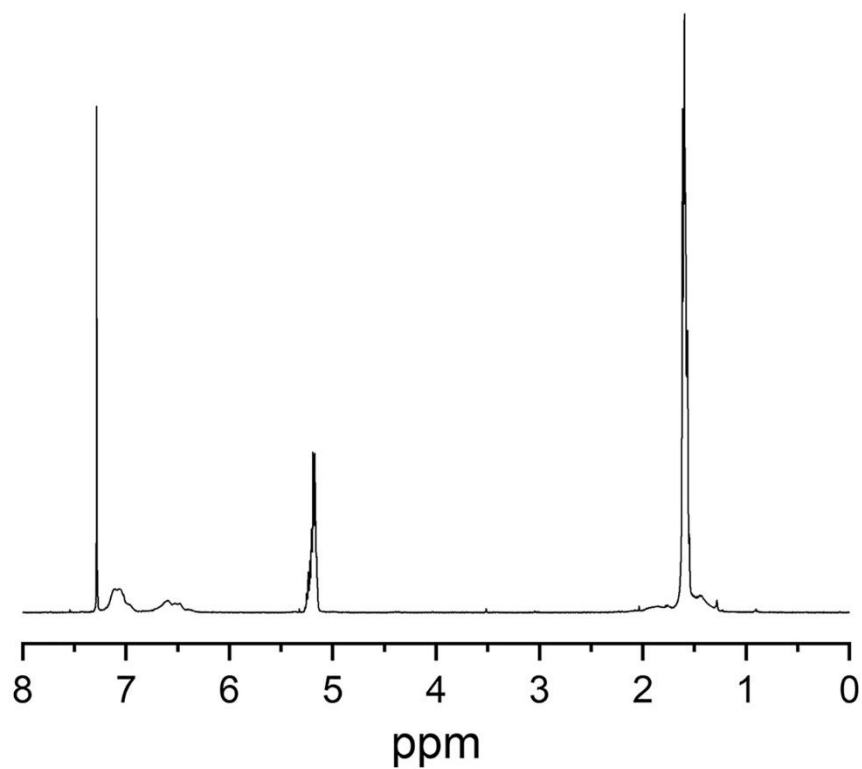


Figure S7. (a)  $^1\text{H}$  NMR spectrum of  $\text{PLA}_n\text{PS}_n(27-7)\text{-MeCN}$  (400 MHz,  $\text{CDCl}_3$ , 20  $^\circ\text{C}$ ).



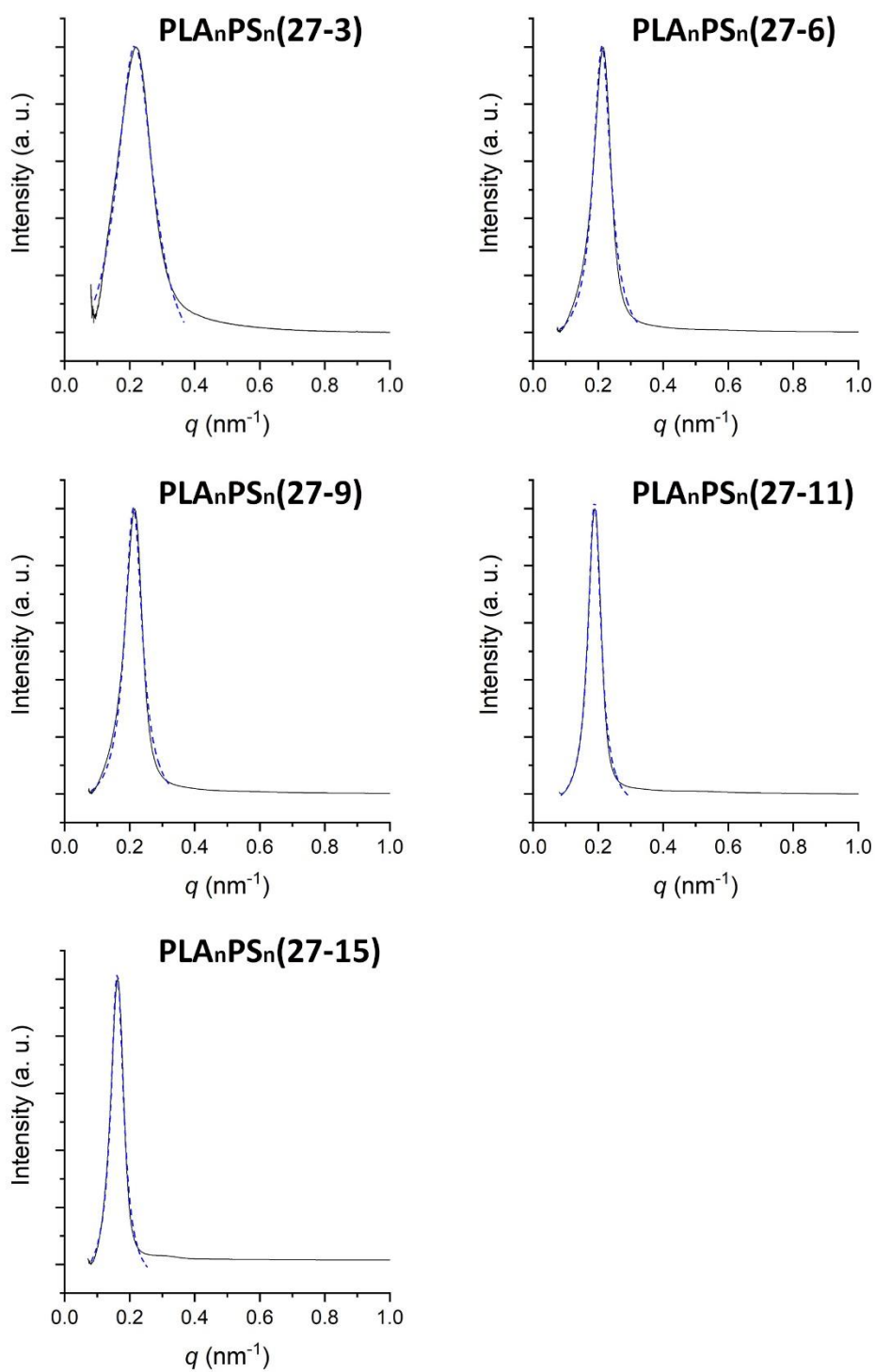


Figure S8. Lorentzian fitting of the SAXS principal peak of PLA<sub>n</sub>PS<sub>n</sub> in toluene. The samples were obtained via the in-out route in DMF. The Lorentzian-fitted peak is shown as a blue dashed line.

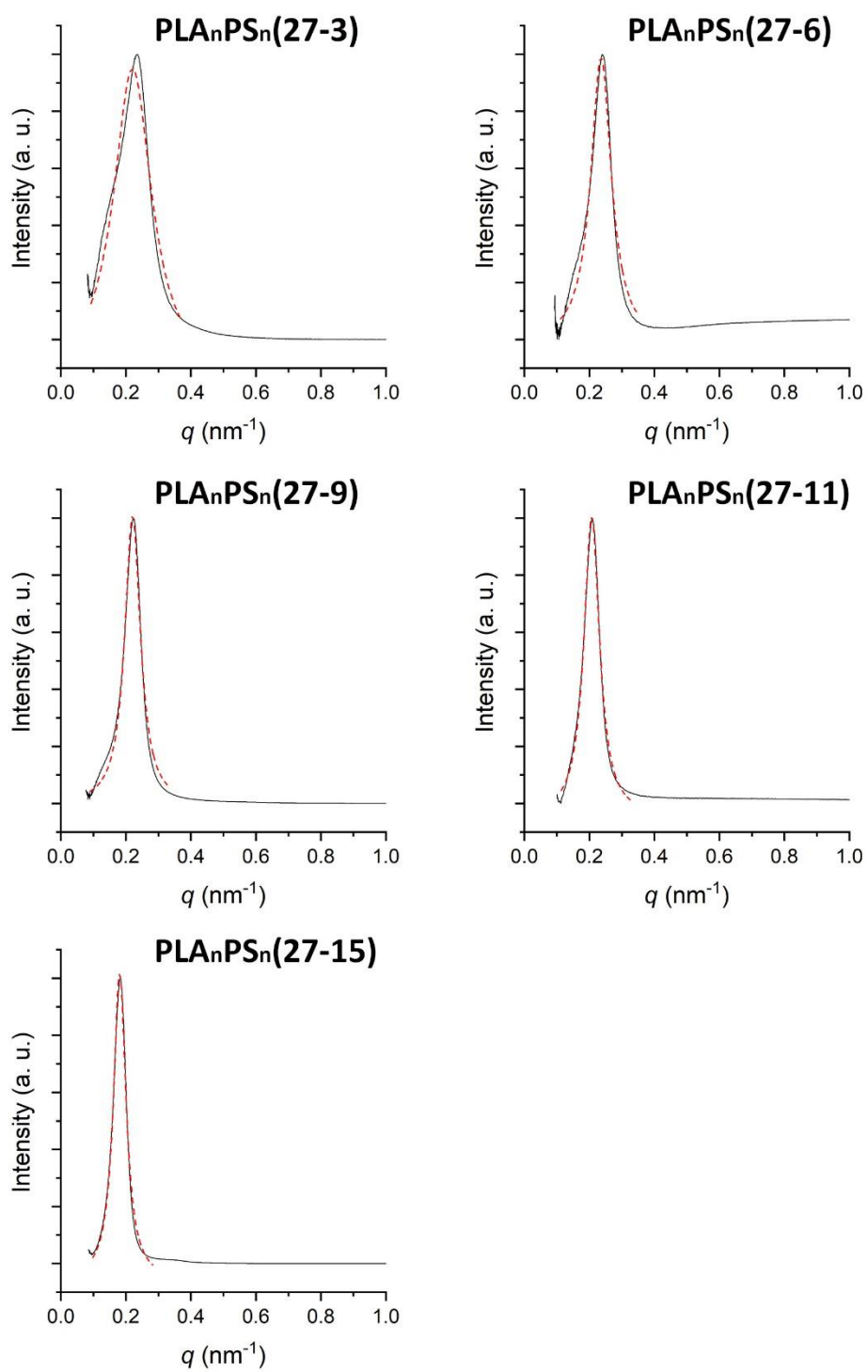


Figure S9. Lorentzian fitting of the SAXS principal peak of PLA<sub>n</sub>PS<sub>n</sub> in acetonitrile. The samples were obtained via the in-out route in DMF. The Lorentzian-fitted peak is shown as a red dashed line.

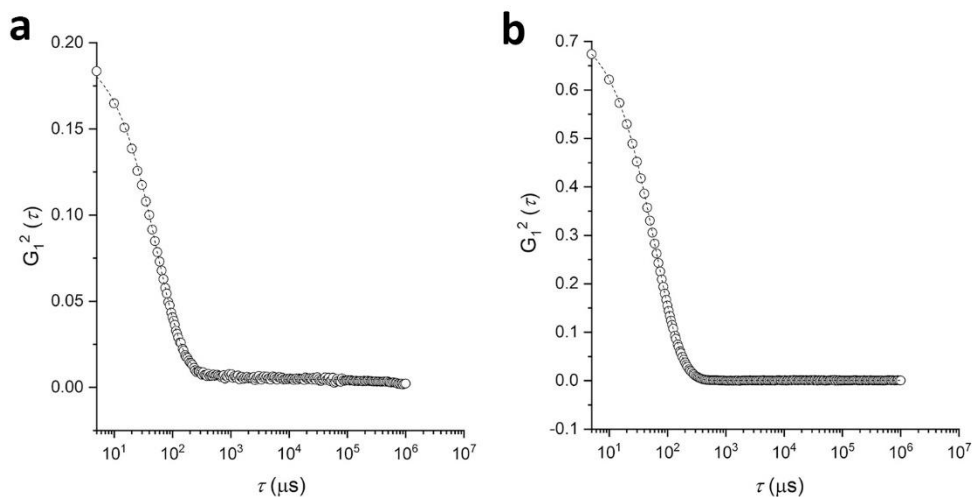


Figure S10. Autocorrelation functions of PLAnPSn(27-13)\_Multi MI in toluene (a) and acetonitrile (b).

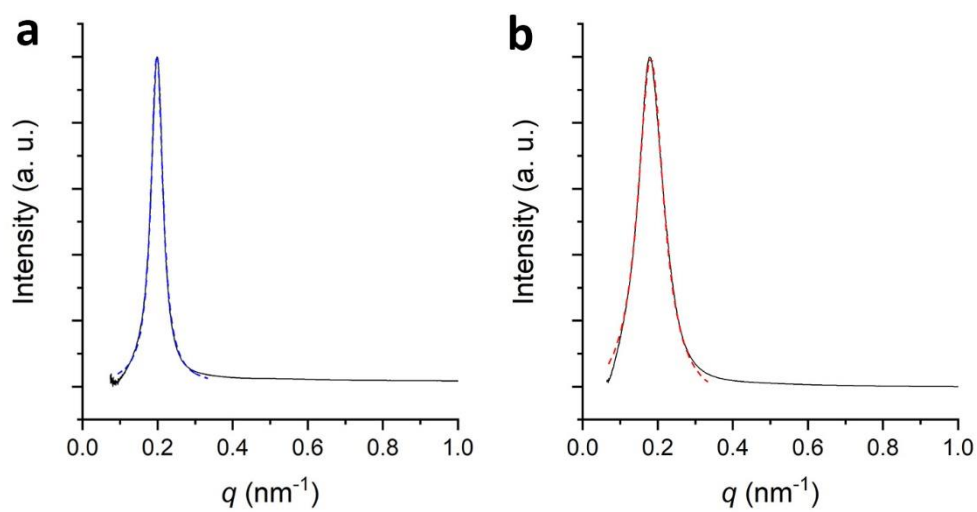


Figure S11. Lorentzian fitting of the SAXS principal peak of PLAnPSn(27-13)\_Multi MI from toluene (a) and acetonitrile (b) solutions. The samples were obtained via the multi MI route in DMF. The Lorentzian-fitted peak is shown as a dashed line.

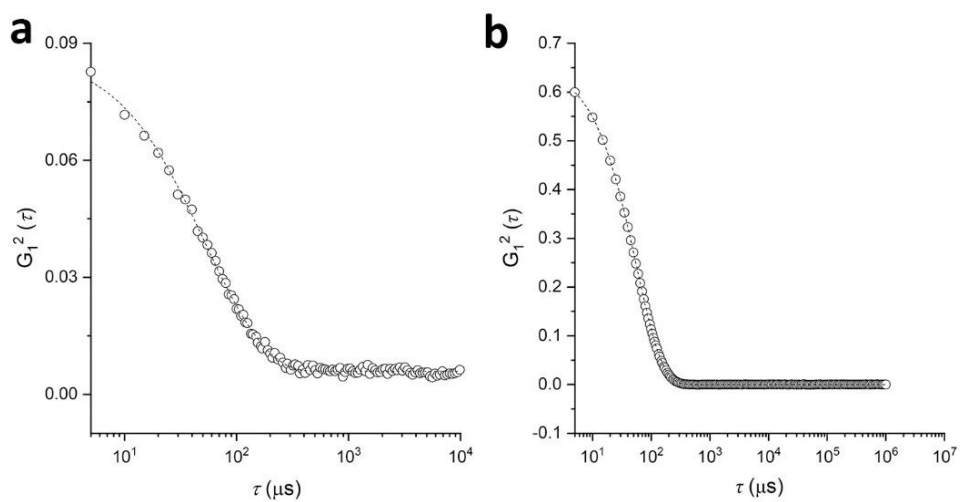


Figure S12. Autocorrelation functions of  $\text{PLA}_n\text{PS}_n(27-7)\text{-MeCN}$  in (a) toluene and (b) MeCN. Concentration of the solutions was  $3 \text{ mg mL}^{-1}$ .

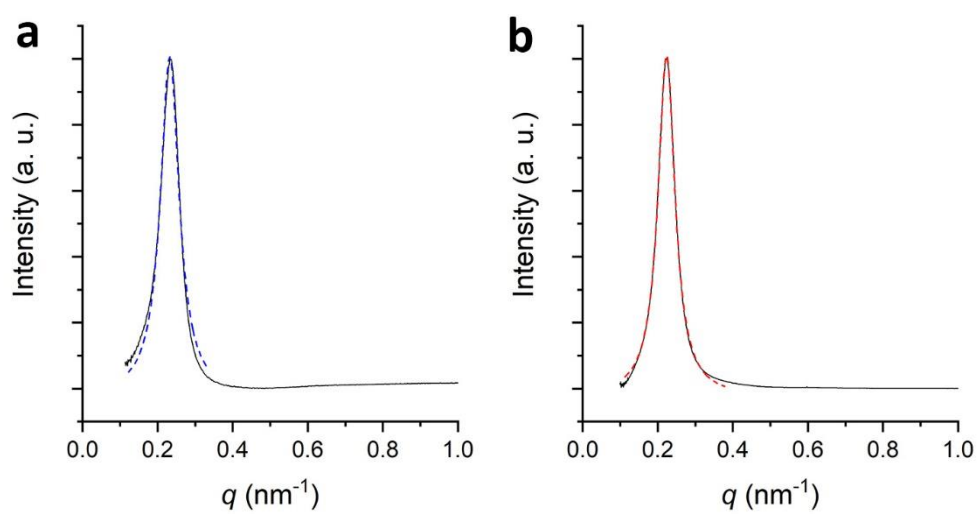


Figure S13. Lorentzian fitting of the SAXS principal peak of  $\text{PLA}_n\text{PS}_n(27-7)\text{-MeCN}$  from toluene (a) and acetonitrile (b) solutions. The samples were obtained via the in-out route in acetonitrile. The Lorentzian-fitted peak is shown as a dashed line.